

Weak ergodicity breaking transition in a randomly constrained modelAydin Deger^{1,2} and Achilleas Lazarides²¹*Department of Physics and Astronomy, University College London, London WC1E 6BT, United Kingdom*²*Interdisciplinary Centre for Mathematical Modelling and Department of Mathematical Sciences, Loughborough University, Loughborough, Leicestershire LE11 3TU, United Kingdom*

(Received 18 October 2023; accepted 23 May 2024; published 11 June 2024)

Experiments in Rydberg atoms have recently found unusually slow decay from a small number of special initial states. We investigate the robustness of such long-lived states (LLS) by studying an ensemble of locally constrained random systems with tunable range μ . Upon varying μ , we find a transition between thermal and weakly nonergodic (supporting a finite number of LLS) phases. Furthermore, we demonstrate that the LLS observed in the experiments disappear upon the addition of small perturbations so that the transition reported here is distinct from known ones. We then show that the LLS dynamics explores only part of the accessible Hilbert space, thus corresponding to localization in Hilbert space.

DOI: [10.1103/PhysRevB.109.L220301](https://doi.org/10.1103/PhysRevB.109.L220301)

Introduction. Isolated quantum systems thermalize: The expectation values of local operators at long times are determined by the values of a small number of conserved quantities (typically, the energy, so that the expectation values coincide with those in the microcanonical ensemble) [1]. This is encapsulated in the eigenstate thermalization hypothesis (ETH) [2,3], which plays the role for quantum systems that the ergodic hypothesis does for classical, forming the bridge between unitary quantum dynamics and statistical mechanics.

Generic systems satisfy ETH as a matter of course [4]. Exceptions robust to weak perturbations include many-body localized systems in the presence of disorder [5–7] (although there is currently debate on whether these are localized or glassy [8–12]) or quasiperiodic potentials [13,14]. Such systems disobey ETH either throughout the spectrum [15] or in a finite fraction of it [16].

Recently, experiments in Rydberg atoms have observed that certain initial conditions result in an abnormally slow decay of the initial state [17]. Consequently, these systems can exhibit a “weak” violation of ergodicity, meaning that a limited number of nonthermalizing eigenstates are present within an otherwise ergodic (thermal) system. This has triggered significant theoretical activity focusing on a class of constrained models, central among them the so-called PXP model [18–24].

In the PXP model, the bulk of the eigenstates satisfies the ETH, but a small number (a vanishing fraction of Hilbert space) violate it—these are called scarred states by analogy to the scarred states discussed in quantum chaos [25]. At the same time they have high overlap with certain experimentally relevant states. Thus, while generic initial

states result in thermalization, starting from one of these few initial states results in the observed anomalous behavior. The central feature of the PXP model explaining this behavior is then to prove the existence of these scarred states.

A pertinent question that arises is the stability of these states when subjected to perturbations. Stability with respect to certain local perturbations has been studied in the following papers: Ref. [26], which found evidence for proximity of the PXP model to an (unknown) integrable model; Ref. [27], which found that the scarred states are unstable (hybridize with the thermal states) in the thermodynamic limit; and Ref. [28], which found that a subset of the scars do remain parametrically stable in the thermodynamic limit. This latter model also studies a translationally invariant modification of the PXP model in which the constraints all have the same tunable range of range α and which hosts a few low-entropy states. The slow decay of the special initial states of PXP disappears, however, once the spatial range of the constraints is increased beyond that of the PXP model [29]. Finally, Ref. [30] studies an ensemble of random Hamiltonians, defined as adjacency matrices of random graphs [31]. While the members of this ensemble only have nonvanishing matrix elements between states differing by a single spin flip, a generic member of the ensemble cannot be written as a sum of local terms—the model is therefore intrinsically nonlocal. Additionally, this work focuses on spectral, rather than dynamical, properties.

In this Letter, we focus on the existence of initial states exhibiting slow decay in models with local PXP-like constraints but of spatially random range. We refer to these states as long-lived states (LLS). We find a phase transition between a fully ergodic (thermal) phase and one with weakly broken ergodicity supporting LLS as the constraint strength μ/N increases above a threshold. The LLS exhibit robust oscillations, returning close to their initial states repeatedly before ultimately decaying. These states are not connected to LLS

Published by the American Physical Society under the terms of the Creative Commons Attribution 4.0 International license. Further distribution of this work must maintain attribution to the author(s) and the published article's title, journal citation, and DOI.

present in the clean PXP model: The latter disappear when we introduce local perturbations to the PXP model, and our LLS only appear once we increase the mean random constraint length. Meanwhile, the bulk spectral properties of the model (such as level statistics) are insensitive to this transition, which is however marked by abrupt changes in both the probability and density of LLS. We finally establish that the LLS in our model are nontrivial, exploring only a small fraction of the accessible Hilbert space.

Our work introduces a class of randomly constrained models that exhibit a distinct form of weak ergodicity breaking in quantum systems. The weak ergodicity breaking we observe is not a consequence of fine tuning, as in the case of the PXP model, but rather emerges robustly due to randomness in kinetic constraints and in the absence of explicit disorder. By demonstrating a dynamical phase transition between a fully ergodic phase and one with weakly broken ergodicity, we establish the existence of distinct phases of weak ergodicity breaking with qualitatively different properties and stability. This finding is significant as it provides numerical evidence of a phase transition in the space of constrained quantum many-body systems. Such transitions may be relevant to recent theoretical discussions about the possibility of scarring phase transition in quantum many-body dynamics [24].

This Letter is organized as follows. We first introduce the model and the class of states in which we are interested, then demonstrate the existence of a phase transition between a fully thermal and a weakly nonergodic phase. This constitutes our main result. We then establish that the LLS explore only a fraction of the accessible Hilbert space, and finally show that the PXP model is an exceptional member of the ensemble we consider—members of the ensemble with the same constraint range as the PXP model but no translational invariance do not support LLS.

Model. Our randomly constrained model is described by the Hamiltonian

$$H = \sum_{i=1}^N X_i \prod_{j=1}^{r_i} P_{i-j} P_{i+j}, \quad (1)$$

where X_i, Z_i are the usual Pauli spin operators and $P_i = (\mathbb{1} - Z_i)/2$ projects to the down (facilitating) state of spin i . Thus, the spin at i can flip only if the $2r_i$ spins a distance r_i on either side are in the facilitating state. We select the r_i independently by drawing random integers from a uniform distribution from interval $[\mu - \epsilon, \mu + \epsilon]$ with a mean μ .

For the model of Eq. (1), as for PXP [32] as well as models displaying Hilbert space shattering [33–35], Fock space breaks up into disconnected components—spin configurations belonging to one are not reachable from the others by repeated action of the Hamiltonian [36]. In this and what follows, we focus on the largest such component of the graph [37]. This sector is always ergodic as far as level statistics and eigenstate properties are concerned [37] but, as we will show, depending on μ , there are nonergodic states.

Our analysis is primarily focused on the return probability, $\mathcal{L}(t) = |\langle \alpha | \exp(-iHt) | \alpha \rangle|^2$ starting from product states $|\alpha\rangle$. We aim to pinpoint those $|\alpha\rangle$ states that exhibit revivals, where the system periodically reverts to a state proximate to its initial configuration. These states will be referred to as

LLS, bearing conceptual resemblance to the two \mathbb{Z}_2 states in the PXP model, which have high overlaps with scarred eigenstates.

In what follows we establish that both the probability that such states exist, p , and their density $\rho = N_{\text{LLS}}/\mathcal{D}_{\mathcal{H}}$ (with N_{LLS} the number of such states and $\mathcal{D}_{\mathcal{H}}$ the dimension of the largest connected component of the Hilbert space) departs from 0 at finite values $\mu_c^{p,\rho}/N$ with N the number of spins; for $\mu < \mu_c^p$ there are no long-lived states, while for $\mu > \mu_c^p$ a finite fraction of Fock states result in long-lived oscillations. Within our numerical analysis, $\mu^{p,\rho}$ appear to be either identical or very close.

At first sight, this appears to contradict known results, since the PXP model is a particular realization of our model for $\mu = 1, \epsilon = 0$ but is known to have LLS. However, we will later show that there is no contradiction: Local perturbations in the PXP model eliminate the scarred states, and consequently its LLS. The LLS we study only appear in the presence of stronger perturbations. Thus our results indicate the presence of a distinct phase with weakly broken ergodicity, unconnected to the one for the PXP model.

Weak ergodicity breaking transition. We use the scaled mean constraining range μ/N as a tuning parameter, varying which (for fixed $\epsilon = 1$) the probability and density of LLS departs from 0 (that is, long-lived states (LLS) appear) at some critical $0.2 \leq \mu_c^{p,\rho}/N \leq 0.3$. We call this transition a *weak ergodicity breaking transition* because it is not visible in the usual ergodicity measures such as level statistics or eigenstate properties [37] but rather is only visible in dynamics starting from a small number of initial states.

To be more concrete, we first provide a precise definition of the LLS and then characterize these states in terms of their strength and persistence. Starting with a given Fock state $|\alpha\rangle$ we evolve it using Eq. (1) up to some time t_{max} and then calculate the return probability $\mathcal{L}(t)$. For α to qualify as a LLS, we count the number of times, N_{th} , that the return probability $\mathcal{L}(t)$ goes above a given threshold \mathcal{L}_{th} . In what follows we define an LLS as one for which $N_{\text{th}} \geq 3$ for $\mathcal{L}_{\text{th}} = 0.5$. We have checked that our main findings are qualitatively the same for other definitions of N_{th} and \mathcal{L}_{th} [37].

Under this definition, the \mathbb{Z}_2 states are categorized as LLS in the PXP model. Consequently, this definition facilitates the connections between LLS and nonthermal many-body states. That is, the presence of LLS for a specified μ implies the existence of eigenvectors that highly overlap with the LLS, giving rise to quantum many-body scarring.

In Fig. 1, we report conclusive evidence of the aforementioned phase transition. Figure 1(a) shows LLS probability for different system sizes as a function of μ/N while Fig. 1(b) shows the density of LLS—the fraction of Fock states in the largest connected cluster that are LLS. Both of these measures depart from 0 at around $\mu/N \approx 0.2$.

For the probability p , the trend in Fig. 1(a) with increasing system size makes it clear that, in the thermodynamic limit, p rapidly rises to 1 above $\mu/N = \mu_c^p/N \approx 0.2$, so that at least one LLS appears. Meanwhile, the density ρ displays a more intricate behavior as depicted in Fig. 1(b). Initially, it too departs from 0 at $\mu/N \approx \mu_c^p/N$ and just above it trends to a finite value as N increases. At $\mu/N > \mu_c^p/N \approx 0.2$, the density increases with system size (see inset), so that one can

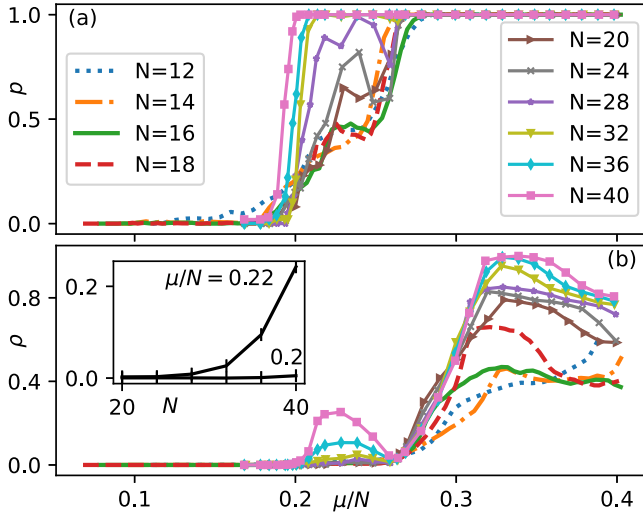


FIG. 1. Weak ergodicity transition. (a) Probability of finding at least one LLS for mean constraint range μ/N ; for $N < 18$ we averaged over 1000 realizations per μ/N and up to time $t_{\max} = 18$, while for $N > 20$ we used 100 realizations up to $t_{\max} = 50$. (b) Density ρ of LLS vs of μ/N jumps sharply away from 0 around $\mu/N \sim 0.2$. The inset shows ρ vs system size N for $\mu/N = \{0.2, 0.22\}$; above $\mu/N \sim 0.2$, ρ increases with system size. We believe the bump between $\mu/N = 0.2$ and 0.3 to be a finite-size effect (see text). This indicates a phase transition in the thermodynamic limit.

confidently state that for $\mu/N > \mu_c^p/N$ a finite density of Fock states are LLS. While there exists a parameter regime $0.2 < \mu/N < 0.3$ where the behavior appears to be nonmonotonic, with two peaks appearing, we believe this to be a finite-size effect for the following reason. In the Supplemental Material [37] we show plots of both p and ρ for different thresholds $\mathcal{L}_{\text{th}} = 0.6$ and 0.7 , larger than the value 0.5 used here. We notice that for $\mathcal{L}_{\text{th}} = 0.6$, the density ρ also picks up this peak for higher values of N . For the probability p at $\mathcal{L}_{\text{th}} = 0.5$ the trough gets filled in above $N \geq 30$ whereas for $\mathcal{L}_{\text{th}} = 0.6$ at $N \geq 40$, so we expect that the trend continues at $\mathcal{L}_{\text{th}} = 0.7$ with the trough getting filled in at a larger N which we cannot access [37]. This suggests again that this is not a few-body effect, as it only appears at large enough sizes. We have not been able to ascertain the origin of this behavior, so that it remains to be determined in future work. Since p is more sensitive than ρ (as it detects a single LLS), we conclude that this behavior will also be mirrored for ρ , but at larger (and inaccessible to us) sizes, and thus believe the actual transition in ρ to lie at the point where it departs 0 for the first time, around 0.2 . In conclusion, from our results in Fig. 1 it is evident that, first, LLS definitely appear for $\mu/N > \mu_c^p/N \approx 0.2$ and, second, that a *finite density* of such states appears for $\mu/N > \mu_c^p/N \approx 0.2$.

Two obvious questions present themselves at this point. First, could it be that the largest connected component in Hilbert space is small enough that we are simply seeing recurrences because of its finiteness (as opposed to the revivals being due to the dynamics exploring only a subspace of that)? Second, from Fig. 1, it would appear that the PXP model, a specific realization of $\mu/N = 1/N$, should display no LLS.

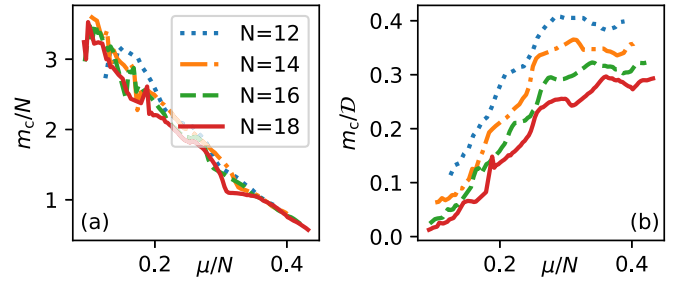


FIG. 2. Minimum number of states m_c required to reproduce the return probability of LLS for a given constraint range μ/N . (a) Scaled by system size N ; m_c/N does not depend on system size, while (b) m_c/D_H decreases with system size, indicating that the *fraction* of Hilbert space that is involved in the dynamics decreases with system size. In both panels, averaging is performed over 1000 realizations for each μ .

But, as is well known, it does have LLS; so how can our results be reconciled with that?

We answer each of these questions in turn.

Truncated Lanczos iterations. In order to address the first question, we analyze the fraction of the Hilbert space of the largest connected component explored by the dynamics starting from the LLS. To do so we use the Lanczos algorithm. In brief, this involves the following steps: Given an initial vector $|\alpha\rangle_0$ and a matrix H , at the n th step one constructs a vector $|\beta_n\rangle = H|\alpha_n\rangle - u_n|\alpha_n\rangle$ with $u_n = \langle\alpha_n|H|\alpha_n\rangle$ and $v_n = \sqrt{\langle\beta_n|\beta_n\rangle}$; then $|\alpha_{n+1}\rangle = |\beta_n\rangle/v_{n+1}$. After m such iterations, one forms the matrix $H_{\text{eff}}(m) = VT V^\dagger$ where V has the $|\alpha_n\rangle$ as columns and T has the u_n on the main diagonal and the v_n on the first off-diagonal constitutes an approximation to H . In principle, $m = \mathcal{D}_H$ exactly reproduces H .

Our approach *truncates* this procedure at some order m , determined by minimizing the following cost function with respect to m :

$$I = \frac{1}{t_{\max}} \min_m \int_0^{t_{\max}} dt |\mathcal{L}(t) - \mathcal{L}_{\text{TLL}}(m, t)|. \quad (2)$$

Here, $\mathcal{L}(t)$ represents the return probability of a LLS evolved with (1), while $\mathcal{L}_{\text{TLL}}(m, t)$ denotes the return probability with an effective Hamiltonian $H_{\text{eff}}(m)$ constructed by using the Lanczos algorithm. We terminate the minimization procedure when $I \leq 0.01$. The aim of this truncation is to determine what fraction of Hilbert space is explored by the dynamics by explicitly constructing it—its dimension is clearly m_c . A similar approach has recently been used to differentiate between localized and chaotic quantum systems [38].

For each realization at a given μ/N , we obtain the m_c for each LLS, then average over all the LLS and realizations. The resulting m_c as a function of μ/N , is shown in Fig. 2, scaled by N (left panel) or \mathcal{D}_H (right panel). Our findings elucidate several key aspects. First, the number of states m_c required is linear in system size N for a given μ/N (left panel), exhibiting a universal behavior. Second, a notable decrease in m_c is observed with increasing constraint range (left panel). Lastly, the *fraction* of the Hilbert space involved in the dynamics for given μ/N decreases with increasing system size (right panel).

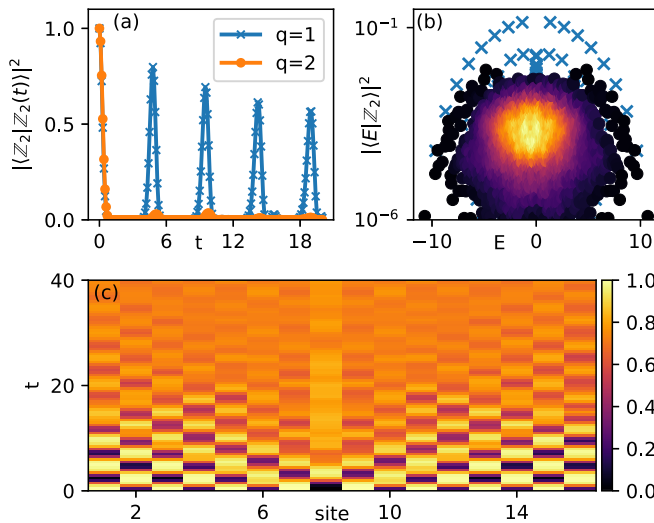


FIG. 3. Scars vanish due to a defect in the constrained range: we set $r_{i_0} = q$ for a single site i_0 , and leave $r_i = 1$ for $r_i \neq i_0$. (a) Return probability starting from the \mathbb{Z}_2 state. $q = 1$ (blue, point) corresponds to the standard PXP model whereas $q = 2$ (orange, square) means that there is a single defect with strength equal to 2. (b) Overlap of the \mathbb{Z}_2 state with the eigenstates. (c) Spatiotemporal profile of density starting from the \mathbb{Z}_2 state with a single defect $q = 2$.

Let us summarize this calculation and the conclusions to be drawn from it. We have shown that the dynamics of the LLS is restricted to a Krylov subspace of a dimensionality that is a decreasing fraction of the dynamically accessible Hilbert space. This implies that the LLS are caused by nontrivial dynamics inside the largest connected cluster, rather than simply a result of the dimension of the largest cluster decreasing with μ/N .

Disappearance and reemergence of quantum scars. We now come to the apparent contradiction mentioned earlier, namely, that in Fig. 1 the probability for LLS to exist for $\mu/N = 1$ vanishes, while the PXP model is a particular realization of $\mu/N = 1/N \rightarrow_{N \rightarrow \infty} 0$. The resolution of this paradox is that the PXP model is a singular point: Changing a single $r_i \neq 1$ results in a rapid decay of the oscillations and destroys the unique spectral structure. Figure 3(a) shows the return probability starting from a \mathbb{Z}_2 state for both standard PXP and for the PXP model modified by setting a single $r_{i_0} = 2$ for some i_0 . In Fig. 3(b), we show the overlap of the \mathbb{Z}_2 state with

the eigenstates of the model for the case of the standard PXP (blue) and our perturbed model with $r_{i_0} = 2$; the characteristic peaks that are known from the PXP model disappear (the same behavior is observed for all other Fock states in the largest sector). Thus, weak, local perturbations of the PXP model disrupt the scars (thus also the LLS, \mathbb{Z}_2 and \mathbb{Z}'_2 in the notation of Ref. [32]), which implies that the phase with LLS that we uncover at higher μ/N is not connected to the scarred phase of the PXP model.

At this point, it is natural to question how a *local* perturbation can disrupt *global* quantities such as the eigenstate overlaps; after all, in the thermodynamic limit, a local perturbation should be negligible, so how is it capable of eliminating the oscillations? The resolution to this paradox is that the eigenstates most directly pertain to infinite-time results of observables via the ETH. Thus, as we show in Fig. 3(c), the oscillations starting from a Néel \mathbb{Z}_2 state with a model with a single $r_{i_0} = 2$ results in oscillations decaying inside a light cone spreading out from i_0 ; only after a time $\propto N$ will they decay everywhere. The effect is visible in spectral properties such as the eigenstate expectation values only because those are relevant for the infinite-time limit.

Conclusion. In this Letter we have studied an ensemble of random, local, constrained models parametrized by the mean constraint range μ . We find that typical members of the ensemble transition from a low- μ/N phase with no LLS to a high- μ/N phase with a high density of LLS. This appears to contradict known results for the PXP model, which is a special case for $\mu = 1$. We reconcile the two results by showing that increasing the constraint range at a single site of PXP causes its unique spectral features to disappear.

A number of open questions on the nature and origins of these LLS remain. Numerical experiments with the Lanczos methods (not shown) suggest that the dynamics of some, but not all, of our LLS is well reproduced by replacing the Hamiltonian by the adjacency matrix of a hypercube with the initial LLS as a node [20]. Can this idea be extended to include all of them? Do all LLS correspond to dynamics on a small number of special subgraphs (analogously to how the PXP LLS are due to adjacency matrices corresponding to a hypercube, or the “motifs” of Ref. [30])? We leave the answers to such questions for future work.

Acknowledgment. We thank J. P. Garrahan for helpful discussions. This work was supported by EPSRC Grant No. EP/V012177/1.

[1] J. von Neumann, Proof of the ergodic theorem and the H -theorem in quantum mechanics, *Eur. Phys. J. H* **35**, 201 (2010).
 [2] J. M. Deutsch, Quantum statistical mechanics in a closed system, *Phys. Rev. A* **43**, 2046 (1991).
 [3] M. Srednicki, Chaos and quantum thermalization, *Phys. Rev. E* **50**, 888 (1994).
 [4] L. D’Alessio, Y. Kafri, A. Polkovnikov, and M. Rigol, From quantum chaos and eigenstate thermalization to statistical mechanics and thermodynamics, *Adv. Phys.* **65**, 239 (2015).
 [5] A. D. Mirlin, Y. V. Fyodorov, F.-M. Dittes, J. Quezada, and T. H. Seligman, Transition from localized to extended eigenstates in

the ensemble of power-law random banded matrices, *Phys. Rev. E* **54**, 3221 (1996).

[6] D. Basko, Hopping between localized Floquet states in periodically driven quantum dots, *Phys. Rev. Lett.* **91**, 206801 (2003).
 [7] R. Nandkishore and D. A. Huse, Many-body localization and thermalization in quantum statistical mechanics, *Annu. Rev. Condens. Matter Phys.* **6**, 15 (2015).
 [8] J. Šuntajs, J. Bonča, T. Prosen, and L. Vidmar, Quantum chaos challenges many-body localization, *Phys. Rev. E* **102**, 062144 (2020).

- [9] P. Sierant, D. Delande, and J. Zakrzewski, Thouless time analysis of Anderson and many-body localization transitions, *Phys. Rev. Lett.* **124**, 186601 (2020).
- [10] D. Sels and A. Polkovnikov, Dynamical obstruction to localization in a disordered spin chain, *Phys. Rev. E* **104**, 054105 (2021).
- [11] D. Abanin, J. H. Bardarson, G. De Tomasi, S. Gopalakrishnan, V. Khemani, S. Parameswaran, F. Pollmann, A. Potter, M. Serbyn, and R. Vasseur, Distinguishing localization from chaos: Challenges in finite-size systems, *Ann. Phys.* **427**, 168415 (2021).
- [12] P. Sierant and J. Zakrzewski, Challenges to observation of many-body localization, *Phys. Rev. B* **105**, 224203 (2022).
- [13] M. Schreiber, S. Hodgman, P. Bordia, H. Lüschen, M. Fischer, R. Vosk, E. Altman, U. Schneider, and I. Bloch, Quantum gases. observation of many-body localization of interacting fermions in a quasirandom optical lattice, *Science* **349**, 842 (2015).
- [14] S. Iyer, V. Oganesyan, G. Refael, and D. A. Huse, Many-body localization in a quasiperiodic system, *Phys. Rev. B* **87**, 134202 (2013).
- [15] D. A. Huse, R. Nandkishore, and V. Oganesyan, Phenomenology of fully many-body-localized systems, *Phys. Rev. B* **90**, 174202 (2014).
- [16] D. J. Luitz, N. Laflorencie, and F. Alet, Many-body localization edge in the random-field Heisenberg chain, *Phys. Rev. B* **91**, 081103(R) (2015).
- [17] H. Bernien, S. Schwartz, A. Keesling, H. Levine, A. Omran, H. Pichler, S. Choi, A. S. Zibrov, M. Endres, M. Greiner, V. Vuletić, and M. D. Lukin, Probing many-body dynamics on a 51-atom quantum simulator, *Nature (London)* **551**, 579 (2017).
- [18] I. Lesanovsky, Many-body spin interactions and the ground state of a dense Rydberg lattice gas, *Phys. Rev. Lett.* **106**, 025301 (2011).
- [19] C. Turner, A. Michailidis, D. Abanin, M. Serbyn, and Z. Papić, Weak ergodicity breaking from quantum many-body scars, *Nat. Phys.* **14**, 745 (2018).
- [20] C. J. Turner, A. A. Michailidis, D. A. Abanin, M. Serbyn, and Z. Papić, Quantum scarred eigenstates in a Rydberg atom chain: Entanglement, breakdown of thermalization, and stability to perturbations, *Phys. Rev. B* **98**, 155134 (2018).
- [21] K. Bull, J.-Y. Desaulles, and Z. Papić, Quantum scars as embeddings of weakly broken lie algebra representations, *Phys. Rev. B* **101**, 165139 (2020).
- [22] K. Bull, I. Martin, and Z. Papić, Systematic construction of scarred many-body dynamics in 1D lattice models, *Phys. Rev. Lett.* **123**, 030601 (2019).
- [23] B. Jeevanesan, Quantum scar states in coupled random graph models, *Phys. Rev. B* **108**, 075131 (2023).
- [24] B. Buča, Unified theory of local quantum many-body dynamics: Eigenoperator thermalization theorems, *Phys. Rev. X* **13**, 031013 (2023).
- [25] E. J. Heller, Bound-state eigenfunctions of classically chaotic Hamiltonian systems: Scars of periodic orbits, *Phys. Rev. Lett.* **53**, 1515 (1984).
- [26] V. Khemani, C. R. Laumann, and A. Chandran, Signatures of integrability in the dynamics of Rydberg-blockaded chains, *Phys. Rev. B* **99**, 161101(R) (2019).
- [27] F. M. Surace, M. Votto, E. G. Lazo, A. Silva, M. Dalmonte, and G. Giudici, Exact many-body scars and their stability in constrained quantum chains, *Phys. Rev. B* **103**, 104302 (2021).
- [28] C.-J. Lin, A. Chandran, and O. I. Motrunich, Slow thermalization of exact quantum many-body scar states under perturbations, *Phys. Rev. Res.* **2**, 033044 (2020).
- [29] J.-Y. Desaulles, K. Bull, A. Daniel, and Z. Papić, Hypergrid subgraphs and the origin of scarred quantum walks in many-body Hilbert space, *Phys. Rev. B* **105**, 245137 (2022).
- [30] F. M. Surace, M. Dalmonte, and A. Silva, Quantum local random networks and the statistical robustness of quantum scars, *SciPost Phys.* **14**, 174 (2023).
- [31] S. Roy and A. Lazarides, Strong ergodicity breaking due to local constraints in a quantum system, *Phys. Rev. Res.* **2**, 023159 (2020).
- [32] C. Turner, K. Meichanetzidis, Z. Papić, and J. Pachos, Optimal free descriptions of many-body theories, *Nat. Commun.* **8**, 14926 (2017).
- [33] P. Sala, T. Rakovszky, R. Verresen, M. Knap, and F. Pollmann, Ergodicity breaking arising from Hilbert space fragmentation in dipole-conserving Hamiltonians, *Phys. Rev. X* **10**, 011047 (2020).
- [34] S. Pai, M. Pretko, and R. M. Nandkishore, Localization in fractonic random circuits, *Phys. Rev. X* **9**, 021003 (2019).
- [35] V. Khemani, M. Hermele, and R. M. Nandkishore, Localization from Hilbert space shattering: From theory to physical realizations, *Phys. Rev. B* **101**, 174204 (2020).
- [36] Viewing the spin model as a single-particle hopping problem on a graph, the adjacency matrix of which is the Hamiltonian, not all sites are reachable by allowed hops from all others.
- [37] See Supplemental Material at <http://link.aps.org/supplemental/10.1103/PhysRevB.109.L220301> for where we describe the construction of the largest connected cluster of the Hamiltonian, display level statistics inside that cluster and show the effect of different LLS thresholds.
- [38] Y. A. Alaoui and B. Laburthe-Tolra, A method to discriminate between localized and chaotic quantum systems, [arXiv:2307.10706](https://arxiv.org/abs/2307.10706).